Time synchronization problem in a multiple wireless ECG sensor measurement

Andrej Vilhar, Matjaž Depolli
Department of Communication Systems, Jožef Stefan Institute, Slovenia
andrej.vilhar@ijs.si,
matjaz.depolli@ijs.si

***Abstract*—The paper addresses the time synchronization of multiple wireless ECG sensors. The approach to the problem is practical, by conducting laboratory experiments on an artificially generated signal. The performed analyses show that the sampling frequency should be followed continuously or the clock drifts will lead to clock offsets in the order of several samples per day. A method has been developed for continuous sampling frequency monitoring. It has been demonstrated to limit the clock drift to about 4 ms (0.5 sample at sampling frequency 125 Hz) over the period of 80 hours.**

***Keywords*—ECG measurement, time synchronisation, wireless sensors.**

I. Introduction

From the beginning of the 20th century, the field of ECG measurement and analysis has matured into today's golden standard 12-lead ECG. Besides the classical stationary multichannel ECG body surface mapping systems [1], ambulatory monitors (the typical representative being Holter monitor) have been used in medicine as portable devices for long-term ECG monitoring since the 1960s [2].

The technological advancements have later enabled the ambulatory monitoring devices to become smaller and to record high-quality ECG signals gathered by a reduced number of electrodes. The recordings are transmitted instantly over the wireless channel to a nearby hub with access to the Internet. The described configuration enables the provision of a wide range of mobile health services, from patient monitoring in hospitals [3], remote patient monitoring [4][5], and remote medical support, to sports, recreation, and entertainment.

A multifunctional ECG wearable sensor device is being developed at Jožef Stefan Institute as a part of an mHealth platform [6]. The device comprises an ECG analog sensing circuitry, micro-controller, and Bluetooth Low Energy (BLE) radio transmitter. It has no storage capacity and very low processing capabilities, keeping it small and energy efficient. It is worn on the chest where it is able to measure ECG and transmit it wirelessly to a smartphone.

The simplicity of the device on one hand enables it to be unobtrusive and as such easily wearable during everyday activities, on the other hand, it imposes several technological challenges. The main challenge is data integrity, which may be compromised due to the inaccurate clock on the sensor side, random delay from the wireless protocol, and to our experience, even due to clock rate variations on the smartphone hub.

The challenge has to be addressed already at the level of a single ECG sensor and has been partially covered in our previous work [7]. Our intension is to advance the system further, by joining correctly the measurements from multiple ECG sensors, measuring the same subject and connected to the same smartphone. The motivation is based on the previously proposed methodologies which demonstrate that classical 12-lead ECG measurements can be synthesized from 3 concurrent differential ECG measurements [8].

The goal of this paper is to analyse the challenges for supporting the 12-lead ECG synthesis from multiple wireless sensors, and to test the methods for accurate synchronization of multiple ECG sensors. Although this paper deals with ECG sensors specifically, it is relevant for synchronization of any kind of high-frequency measurements from multiple sources with separate clocks.

The paper is organized as follows. In the next section, the problem is stated, by separating it to sub-problems. The proposed method is presented in Section III and evaluated in Section IV. The paper concludes in Section V.

II. Problem Statement

Keeping accurate time, which is required for synchronizing events measured on different devices, is not trivial. The wearable ECG sensor is a simple device with internal representation of time depending purely on the quartz oscillator, which is estimated to be accurate to under 100 ppm [9]. If the inevitable clock drift is not properly compensated, it can amount to several seconds during one week of measurement. While such accuracy is perfectly acceptable for long-term ambulatory ECG measurement performed by a single sensor, it is not acceptable for the application of data fusion from multiple concurrent measurements. To support the 12-lead ECG synthesis, a very strict synchronization demand is imposed, for the timing precision to be within several milliseconds, which can be below a single sampling period.

The synchronization of multiple sensors is achieved by compensation for the clock drift at the controller node,

ISBN 978-3-903176-02-7

performed independently for each of the sensors. However, the real challenge is hidden in practical implementation, which has to confront two major limitations. These are the uncertainty and variable delay on the communication channel, and the clock rate variations between the nodes of the system.

A. Single sensor synchronization

The problem of communication channel uncertainty is addressed at the level of a single sensor time synchronization. A custom protocol on top of the BLE is utilised for wireless data transmission. As a communication protocol, it does not guarantee successful transmission of packets nor the time of their arrival. Delays are caused by the waiting times in buffers on the transmitting and receiving ends, as well as by transition time between the physical OSI layer and the application layer. The packets may thus be lost or come delayed with a certain delay spread, which results in non-equidistant or even missing samples at the controller node.

The anomalies are classified as random delay, packet clusters, packet loss and idle time. The listed anomalies are explained in more details in [7], where also a four-step algorithm was proposed to handle them.

In one of the steps of the algorithm, the sampling frequency is estimated by linear regression. The procedure returns a linear function, expressing the relation between the packet counter marked on the sensor's side and the timestamp at the receiving side. The slope of the function reflects the sampling frequency *fs*. The sampling times of the packets are then determined by projecting them to the line using their sensor device time. If the *fs* is estimated correctly then the time synchronization is accurate. In case of an error in estimation, time deviation increases over time. Estimation of *fs* thus plays a crucial role.

B. Multiple sensors synchronization

The method proposed in [7] seems to perform satisfactory for a single device. It was suspected, however, that it would not suffice for keeping multiple sensors synchronized. In order to quantitatively evaluate the actual level of non-synchronism in a measurement with multiple ECG sensors, laboratory experiments were performed. An artificial ECG signal was generated and measured simultaneously with up to three ECG sensors, connected to the same smartphone. In order to increase the reliability of the results, series of measurements were performed with the same configuration, but different hardware selection, i.e. various models of smartphone devices and different sensor devices of the same model. The source signal remained the same in all cases. The declared sampling frequency for all sensor devices was 125.0687 Hz.

The worst case among the performed experiments with 3 sensors is chosen for demonstration of the impact of *fs* estimation on the measurements. The duration of the test was 7 days. The *fs* was estimated by using three different strategies:

A. *fs* equals the declared sensor sampling frequency,

B. *fs* is estimated by the linear regression on the biggest chunk of correctly received packets,

C. *fs* is estimated by the linear regression on the first 12 hours of received packets.

In all three cases, the estimated sampling frequency was considered to be constant throughout the measurement. At the beginning of the test, the three signals were perfectly aligned. As the time passed, the signals obtained by the strategies A and B become quickly and obviously misaligned, while the strategy C seemed to preserve synchronism. After about 2 days, the three signals obtained by the strategy C also became increasingly misaligned as depicted in Fig. 1.

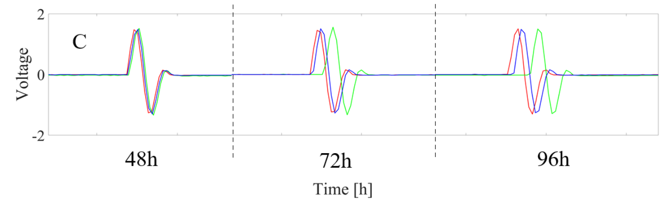

Fig. 1. Non-synchronism of the signals obtained by the strategy C.

Time variations of sampling frequencies during the performed test were analysed further. For each of the three measurement sets, frequency was estimated once per hour, using linear regression over that hour, as defined in single sensor synchronization. Plot of the resulting *fs* as a function of time is given in Fig. 2.

The graph shows that the estimated sampling frequency (solid lines) varies notably with time, up to 0.001 Hz. The deviation seems low in absolute terms, but at the nominal sampling rate *fs* = 125 Hz, this means that the number of collected samples over the period of one day will differ by nearly 90. Therefore, it has to be properly compensated for, especially in the case of multiple signals. The graph shows also the constant *fs* values, estimated by the strategies B and C. The *fs* according to the strategy A is not shown in the graph, because its value is much larger than all the others, 125.0687 Hz.

The *fs* variations of the three signals seem to be well synchronized, with the jumps in estimated frequency occurring at identical times – at around 44 h and 138 h. These are the times when the smartphone display was turned on and off, respectively. This leads us to the logical conclusion that the cause of the observed behaviour originates on the smartphone, not on sensors.

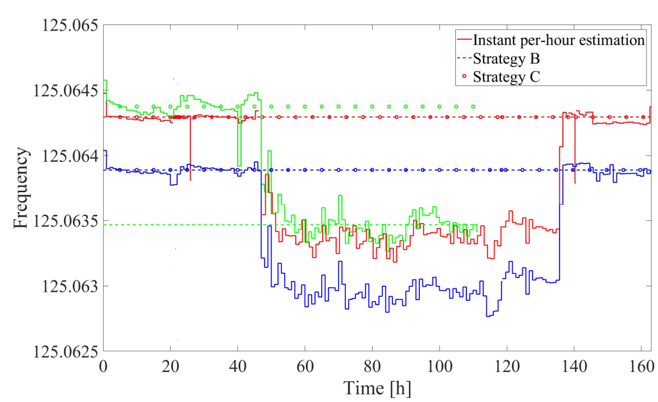

Fig. 2. Estimated sampling frequencies.

Regardless of the cause for the clock drift, unless the *fs* variations are detected and compensated for, the measured signals shall lose synchronization in time. The conclusion is neither surprising nor new, however it has not been quantitatively evaluated in practice before.

III. Methodology

A method has been implemented, which synchronises measurements from multiple ECG sensors with an error below 1 sample. It is based on the assumption that the sensors will remain synchronised as long as the *fs* variations for each of them are detected quickly enough and reacted to at the controller node. The method is built on top of the four-step algorithm [7], with the main difference in the approach to *fs* estimation. Instead of a single constant value, the estimated *fs* keeps changing throughout the measurement. The steps of the algorithm are modified but their number remains to be four.

A. Step 1: Correction of sensor-based counters

The sensors in-use employ 10-bit sample counters for tracking and reporting sample times, thus an overflow occurs on every 1024th sample, i.e., once every 8 seconds. The sample times are extended on the controller side to a 64-bit format by a simple procedure described in [7].

B. Step 2: Signal decomposition

The signal decomposition consists of quality decomposition and frequency decomposition. Quality decomposition aims to partition the measurements into good and bad blocks, where the latter contain hard to compensate flaws, such as missing packets, delayed packets or idle time. All these flaws can be recognised from the longer than usual time difference between consecutive received packets. The procedure flags blocks of packets as good where the time interval Δt_i between each of the packet pairs i is less than 60 times the nominal sampling time. Good blocks are therefore those that only contain packets with time differences up to about 0.5 s. Since frequency will later be estimated on good blocks, it is important that they hold enough packets. Therefore additional rule is introduced that requires the length of a good block to be at least $4000 \cdot T_S$, which is about 30 s. Parts of the measurements that do not qualify as good blocks are designated as bad blocks.

The threshold values listed above were determined empirically, based on several trials performed on measurements with obvious irregularities. The values should be adjusted in the future by researching what works best on a larger sample of measurements.

The second task of this step is further splitting the good blocks into smaller blocks of predetermined maximum length, typically in the order of a few minutes. The motivation behind the task is to improve granularity of sampling frequency estimation, which shall take place in the next step, to compensate for the clock drift.

C. Step 3: Processing individual blocks

Each individual good block undergoes a simple linear regression [10]. That is, it fits a straight line in the scatter plot of counter versus reference time, which minimizes the sum of squared residuals. The intercept of the line is determined according to the sample with highest absolute error among the errors with negative error. This guarantees the estimated timestamps of all the samples are lower or equal to measured timestamps, since we know that measured timestamps are sample times plus an unknown but positive delay.

The bad blocks should be discarded and their further processing is not recommended. Nevertheless, a linear line is determined for them, based on a simple linear regression performed beforehand on the largest good block.

D. Step 4: Sampling time estimation

In the last step, the estimated sampling frequencies, determined on each of the signals blocks, are used to derive sampling times of all the packets. For each of the packet, the sampling time is determined as:

$$t_i = \frac{c_i - c_0}{f_s},$$

where c_i is the value of the counter for that packet, while c_0 and *fs* are the intercept and the slope, respectively, determined in the previous step, separately for each block.

IV. Evaluation

The proposed methodology is evaluated on the same experimental dataset as presented in Section II. The method is referred to as the strategy F, denoting the fact that it is based on constant monitoring of the sampling frequency. The time window for *fs* estimation was chosen to be 1 hour.

As depicted in Fig. 3, the three signals obtained by the strategy F are kept well aligned even after 96 hours of operation. A slight offset of about half a sample is observed after 72 hours, but the difference seems to diminish again at the end of observation. In comparison to the best of the strategies with constant *fs* (strategy C), the improvement is obvious.

The presented comparison shows how the three signals are aligned at selected moments of time. It fails however to quantitatively evaluate synchronism throughout the experiment. A new metric is introduced for this purpose. The algorithm for evaluation finds the peaks of the three signals and compares their timing once per hour. A pairwise comparison between the signals is performed with the time difference among the closest pairs of peaks calculated.

The metric is calculated for the first 110 hours, which is the total duration of all the three signals measured in parallel. The comparison among the signal pairs as obtained by the best two strategies, C and F, is shown in Fig. 4 and Fig. 5, respectively.

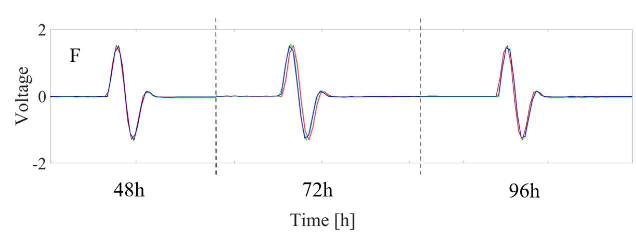

Fig. 3. Signals obtained using the proposed synchronization procedure.

ISBN 978-3-903176-02-7 © 2018 IFIP

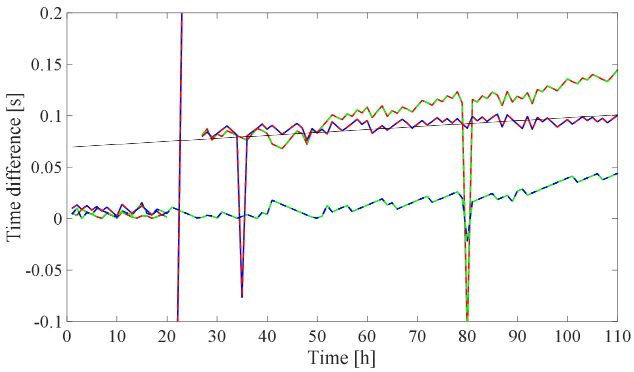

Fig. 4. The time difference metric obtained after applying the strategy C.

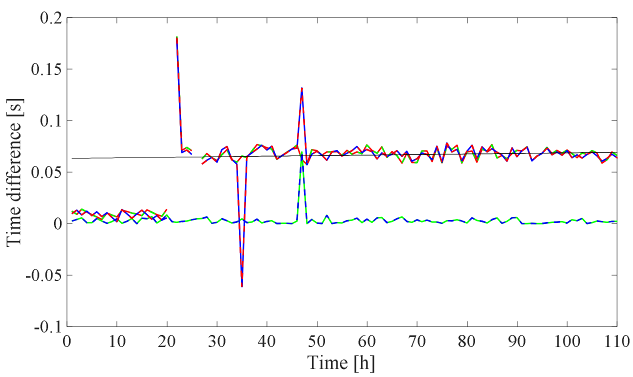

Fig. 5. The time difference metric obtained after applying the strategy F.

In both figures, an irregular behaviour can be seen at the interval 20 h – 27 h. It is caused by hardware issue of the red signal, and has yet unhandled effects on the measurement. This behaviour introduces a 0.07 s of clock offset at 27h. This issue remains to be addressed systematically in our future work. We corrected the offset manually only for the purpose of the time drift analysis in Fig. 1 and Fig. 3.

A. Strategy C

Among the three strategies with constant *fs*, the strategy C performs the best. Nevertheless, it is affected by clock drifts, as observed in V. The worst pairs are those in combination with the green signal. For example, during the time period 30 h – 110 h, an offset of about 0.06 s (~ 7.5 samples) accumulates for the green-red pair. The best performing pair is the blue-red pair, with an offset of 0.025 s (~ 3 samples).

An interesting behaviour can be observed in the same graph. Even if the *fs* estimations under the strategy C suddenly become notably wrong after 50 h of observation, this does not have a very significant impact on the trend of the observed time differences. The reason lies in the fact that the *fs* changes were similar for the three signals: they happened at the same time and their magnitudes were nearly the same, hence the differences between the actual *fs* and the estimated *fs* remained similar. Nevertheless, the clock drifts are detected and can be ascribed to clock rate variations among the sensor nodes. Consequently, in order to achieve higher accuracy, they have to be properly compensated all the time.

B. Strategy F

The results shown in Fig. 5 confirm that this is possible by applying the strategy F. All the three pairs of signals perform about the same, with nearly unnoticeable offset accumulation over the observed period of time. The inclination of the interpolated line for the blue-red pair is an order of magnitude lower compared to the strategy C. In the time period 30 h – 110 h, an offset of about 0.004 s accumulates, which corresponds to only half a sample discrepancy in 80 hours.

V. Conclusion

The time synchronisation procedure in a wireless sensor application has to be systematic and has to properly address two main issues, (i) the uncertainty and variable delay on the communication channel and (ii) clock rate variations of the sensor and the controller node. The latter seems to be more demanding, especially in ECG measurements, where the error below a single sampling period is required. By comparison of different methodologies it has been shown that the approach with a simple linear regression can be adequate, provided that it is performed continuously, so that the changes of sampling frequency are properly detected and compensated for.

While the continuous sampling frequency estimation is an adequate method for keeping the clock drift effects at minimum, additional clock offsets may arise randomly as a consequence of unpredictable problems in device operation or in communication. Such offsets have to be properly detected and corrected. The task may not always be trivial in practice and hence its development is the matter of our future work.

References

[1] R. Trobec, “Computer analysis of multichannel ECG,” in *Comput. Biol. Med.*, vol. 33, no. 3, pp.215–226, May 2003.

[2] J. Janousek, “Various systems of long-term ECG (Holter) monitoring in clinical practice,” in *Cas. Lek. Cesk.,* vol. 128, no. 14, pp. 429-432, 1989.

[3] P. Bifulco, M. Cesarelli, A. Fratini, M. Ruffo, G. Pasquariello, and G Gargiulo, “A wearable device for recording of biopotentials and body movements,” in *Proc. IEEE Int. Workshop on Medical Measurements and Applications* (MeMeA), pp. 469–472, 2011.

[4] A. Pantelopoulos and N. G. Bourbakis, “A Survey on Wearable Sensor-Based Systems for Health Monitoring and Prognosis,” in *IEEE Transaction on Systems*, vol. 40, no. 1, 2010.

[5] M. Lindén and M. Björkman, “Embedded sensor systems for health - providing the tools in future healthcare,” in *Stud. Health Technol. Inform.*, vol. 200, pp.161–163, 2014.

[6] M. Depolli, V. Avbelj, R. Trobec, J. M. Kalisnik, T. Korosec, A. Poplas Susic, U. Stanic, and A. Semeja, “Pcard platform for mhealth monitoring,” in *Informatica*, vol. 40, no. 1, pp. 117-124, 2016.

[7] A. Vilhar and M. Depolli, “Synchronization of time in wireles ECG measurement,” in *Proc. 40th Jubilee International Convention MIPRO*, Opatija, Croatia, pp. 311-315, May 2017.

[8] I. Tomašić and R. Trobec, “Electrocardiographic systems with reduced numbers of leadssynthesis of the 12-lead ECG,” in *IEEE Reviews in Biomedical Engineering*, vol. 7, pp.126–142, 2014.

[9] C. S. Lam, “A review of the recent development of MEMS and crystal oscillators and their impacts on the frequency control products industry,” in *Proc. IEEE Int. Ultrasonics Symposium*, pp. 694–704, 2008.

[10] Simple linear regression, online description, *Wikipedia.org*, last access October 2017.

ISBN 978-3-903176-02-7